



Cite as: H. Williams *et al.*, *Science* 10.1126/science.adf5307 (2023).

A magnified compact galaxy at redshift 9.51 with strong nebular emission lines

Hayley Williams^{1*}, Patrick L. Kelly¹, Wenlei Chen¹, Gabriel Brammer², Adi Zitrin³, Tommaso Treu⁴, Claudia Scarlata¹, Anton M. Koekemoer⁵, Masamune Oguri^{6,7}, Yu-Heng Lin¹, Jose M. Diego⁸, Mario Nonino⁹, Jens Hjorth¹⁰, Danial Langeroodi¹⁰, Tom Broadhurst¹¹, Noah Rogers¹, Ismael Perez-Fournon^{12,13}, Ryan J. Foley¹⁴, Saurabh Jha¹⁵, Alexei V. Filippenko¹⁶, Lou Strolger⁵, Justin Pierel⁵, Frederick Poidevin^{12,13}, Lilan Yang¹⁷

¹Minnesota Institute for Astrophysics, University of Minnesota, Minneapolis, MN 55455, USA. ²Cosmic Dawn Center, Niels Bohr Institute, University of Copenhagen, DK-2200 Copenhagen, Denmark. ³Physics Department, Ben-Gurion University of the Negev, Beer-Sheva 8410501, Israel. ⁴Department of Physics and Astronomy, University of California, Los Angeles, CA 90095, USA. ⁵Space Telescope Science Institute, Baltimore, MD 21218, USA. ⁶Center for Frontier Science, Chiba University, Chiba 263-8522, Japan. ⁷Department of Physics, Chiba University, Chiba 263-8522, Japan. ⁸Instituto de Física de Cantabria, Universidad de Cantabria, Consejo Superior de Investigaciones Científicas, 39005 Santander, Spain. ⁹Istituto Nazionale di Astrofisica, Osservatorio Astronomico di Trieste, 34124 Trieste, Italy. ¹⁰Dark Cosmology Center, Niels Bohr Institute, University of Copenhagen, DK-2200 Copenhagen, Denmark. ¹¹Donostia International Physics Center, Ikerbasque Foundation, University of the Basque Country, 20018 Donostia, Spain. ¹²Instituto de Astrofísica de Canarias, E-38205 La Laguna, Tenerife, Spain. ¹³Departamento de Astrofísica, Universidad de La Laguna, 38206 La Laguna, Tenerife, Spain. ¹⁴Department of Astronomy and Astrophysics, University of California Observatories/Lick Observatory, University of California, Santa Cruz, CA 95064, USA. ¹⁵Department of Physics and Astronomy, Rutgers, The State University of New Jersey, Piscataway, NJ 08854, USA. ¹⁶Department of Astronomy, University of California, Berkeley, CA 94720-3411, USA. ¹⁷Kavli Institute for the Physics and Mathematics of the Universe, The University of Tokyo, Kashiwa 277-8583, Japan.

*Corresponding author. Email: will5099@umn.edu

Ultraviolet light from early galaxies is thought to have ionized gas in the intergalactic medium. However, there are few observational constraints on this epoch, due to the faintness of those galaxies and the redshift of their optical light into the infrared. We report the observation, in James Webb Space Telescope (JWST) imaging, of a distant galaxy that is magnified by gravitational lensing. JWST spectroscopy of the galaxy, at rest-frame optical wavelengths, detects strong nebular emission lines due to oxygen and hydrogen. The measured redshift is $z = 9.51 \pm 0.01$, corresponding to 510 million years after the Big Bang. The galaxy has a radius of $16.2^{+4.6}_{-7.2}$ parsecs, substantially more compact than galaxies with equivalent luminosity at $z \sim 6$ to 8, leading to a high star formation rate surface density.

Radiation from early galaxies is thought to be responsible for the reionization of the Universe, the process in which the majority of the intergalactic neutral gas was ionized by high energy photons. Observational constraints suggest that reionization was completed when the Universe was approximately one billion years old (redshift $z \sim 6$) (1). The precise timeline of reionization, and the relative contributions of faint and bright galaxies to the ionizing photon budget, remain uncertain (2). Observations of distant galaxies that existed during the epoch of reionization provide information on the physical processes that occurred during that period (3).

The intrinsic faintness and small angular sizes of galaxies at high redshift limit our ability to observe them in detail. Due to their very large masses, galaxy clusters act as gravitational lenses, magnifying the flux and stretching the angular extent of distant background galaxies. Gravitational lensing can therefore extend the observational limits of a telescope, probing faint and small galaxies at high redshifts that would otherwise be undetectable (4).

Near-infrared imaging has identified distant galaxy candidates at $z \gtrsim 9$ and up to $z \approx 17$ (5–7), but the redshifts of those candidates have not been confirmed with spectroscopy.

Among these candidates are an unexpectedly large number of galaxies with bright ultraviolet (UV) absolute magnitudes ($M_{\text{UV}} \lesssim -21$ mag; (8–10)) and high stellar masses ($M_* > 10^{10}$ solar masses (M_\odot); (11)). This population was not predicted by simulations of early galaxy formation that assumed standard cosmology (12, 13). Spectroscopy is necessary to confirm the redshifts of these galaxies and infer their physical properties, from the strengths of their emission lines.

Nebular emission lines are produced by clouds of interstellar gas within a galaxy; spectroscopic analysis of these lines can provide information about the density, temperature, and chemical composition of the gas. Spectroscopy has confirmed three high-redshift galaxies ($7.66 < z < 8.50$) with detections of strong nebular emission lines (14) and the temperature-sensitive [O iii] 4363 Å emission line, which has been used to make direct electron temperature oxygen abundance measurements in galaxies at these redshifts (15–19). There has been further spectroscopic confirmation of seven galaxies from $z = 7.762$ to 8.998 (20).

Imaging observations and analysis

We observed the galaxy cluster RX J2129.6+0005 (hereafter RX J2129) on 2022 October 6 using the Near-Infrared Camera (NIRCam) instrument on JWST, operating in imaging mode as part of a director's discretionary time program (number DD 2767; PI P. Kelly). NIRCam is sensitive to wavelengths in the range 0.6 μm to 5.0 μm ; we obtained exposures in the F115W, F150W, F200W, F277W, F356W, and F444W filters (the name of each filter indicates its approximate central wavelength and bandwidth - for example, the central wavelength of the F115W filter is approximately 1.15 μm and it has a wide bandwidth of 0.225 μm). Our exposure times ranged from 2026 s for the F444W filter to 19,927 s for the F150W filter. The astrometric alignment for the NIRCam images was performed using a catalog prepared from previous imaging taken with the Suprime-Cam instrument on the Subaru telescope (21).

The color-composite NIRCam image of the RX J2129 cluster is shown in Fig. 1. In this image, we identified a candidate distant galaxy (which we designate as RX J2129-z95) which appears as three images due to the gravitational lensing of the foreground cluster. Coordinates for the three images, designated RX J2129-z95:G1, RX J2129-z95:G2, and RX J2129-z95:G3 (hereafter G1, G2 and G3), are given in Table S2. Photometric measurements from the NIRCam imaging, along with measurements from previous Hubble Space Telescope (HST) imaging of the RX J2129 cluster field obtained with the Advanced Camera for Surveys (ACS) and the Wide Field Camera 3 (WFC3), are listed in Table S1 (21).

We used the Eazy-py software (22) to constrain the photometric redshift (an estimate for a source's redshift made without the use of spectroscopy) for all sources in the field detected in the NIRCam imaging (21). We obtained a photometric redshift of $z_{\text{phot}} = 9.38^{+0.29}_{-0.15}$ for image G2 of RX J2129-z95. From the NIRCam photometry, we estimate a UV spectral slope (β) of -1.98 ± 0.11 (21). Using the F150W photometric flux measurement, and correcting for the effect of magnification due to gravitational lensing of image G2 (magnification $\mu = 20.2 \pm 3.8$ (21)), we calculate the absolute UV magnitude at 1500 Å $M_{\text{UV}} = -1.72 \pm 0.22$ mag.

We used the Prospector software (23) to infer the physical properties of the galaxy from the spectral energy distribution (SED) of image G2, using the NIRCam photometry and non-detections from archival optical HST imaging (21). Before doing so, we corrected the photometry for the effect of magnification due to gravitational lensing. We find that the galaxy has a low stellar mass $\log(M_*/M_{\odot}) = 7.63^{+0.22}_{-0.24}$ (uncertainty is 1σ and includes the propagated uncertainty in magnification). The template fitting also indicates an oxygen abundance of $12 + \log(\text{O/H}) = 7.63^{+0.07}_{-0.05}$. The best-fitting star

formation history (SFH) has a mass-weighted age of 56^{+43}_{-34} Myrs and indicates a star formation rate (SFR) of $\text{SFR} = 0.9 \pm 0.32 M_{\odot} \text{ yr}^{-1}$. The observed SED of image G2 and best fitting Prospector model are shown in Figure S3.

We use the Lenstrut software (24, 25) to reconstruct the F150W image of G2, correcting for the effects of gravitational lensing and the NIRCam point spread function (PSF). We fitted the reconstructed image with a surface brightness model, consisting of an elliptical Sérsic profile with index n fixed to 0.5 (n determines the degree of curvature of the profile, with $n = 0.5$ being a Gaussian profile). This indicates the intrinsic half-light radius of the reconstructed source is $R_{\text{e,intrinsic}} = 16.2^{+4.6}_{-7.2}$ parsecs (pc) (Figure S7). We also fitted the observed F150W image directly, using the Galight software (26), which indicates an observed angular size of $\Theta_{\text{e,observed}} = 0.04 \pm 0.01$ arcseconds (21).

Spectroscopic Observations and Analysis

We obtained follow-up spectroscopy of the RX J2129 cluster field on 2022 October 22, using JWST's Near Infrared Spectrograph (NIRSpec) in multi-object spectroscopy (MOS) mode. Targets were selected based on photometric redshift estimates from the NIRCam imaging. We used a standard 3-shutter dither pattern and obtained a 4464 s exposure using the prism disperser. This setup provides wavelength coverage from 0.6 μm to 5.3 μm , with spectral resolving power R ranging from ≈ 50 to ≈ 400 (27). The fully calibrated (21) one-dimensional (1D) and two-dimensional (2D) spectra are shown in Fig. 2.

We estimated the spectroscopic redshift of the galaxy by visual identification of the emission lines H β and [O iii] 4959,5007 Å. We refined our redshift measurement by modeling the emission-line profiles (see below), which yields $z_{\text{spec}} = 9.51 \pm 0.01$. This spectroscopic redshift is consistent with the photometric redshift derived above ($z_{\text{phot}} = 9.38^{+0.29}_{-0.15}$), indicating that the lines have not been misidentified.

To constrain the fluxes of the emission lines, we use the pPXF (Penalized Pixel-Fitting) software (28), which models the stellar continuum and fits Gaussian profiles to each of the emission lines (21). Table 1 lists our measured emission-line fluxes, equivalent widths (EWs), and corresponding uncertainties. We do not detect the Ly α line of hydrogen, with a 3σ upper limit for its flux of approximately 39×10^{-19} erg s^{-1} cm^{-2} (21). We assume negligible extinction due to dust and apply no reddening correction to the flux measurements (21).

We infer the star-formation rate (SFR) of the galaxy from our H β flux measurement using the relation

$$\text{SFR}/(M_{\odot} \text{year}^{-1}) = 5.5 \times 10^{-42} L(\text{H}\alpha)/(\text{erg s}^{-1}) \quad (1)$$

where $L(\text{H}\alpha)$ is the intrinsic $\text{H}\alpha$ luminosity of the galaxy. To compute $L(\text{H}\alpha)$, we correct for magnification due to lensing and assume Case B recombination (29). We find $SFR = 1.69_{-0.34}^{+0.51} M_\odot \text{ yr}^{-1}$ (21). This value is approximately 50% larger than the value we derived above from the SED ($0.90 \pm 0.32 M_\odot \text{ yr}^{-1}$), but the discrepancy is $<2\sigma$. Using the stellar mass we inferred from the SED ($\log(M_*/M_\odot) = 7.63_{-0.24}^{+0.22}$), we compute the specific star formation rate (sSFR, the SFR per unit mass), finding $\log(\text{sSFR}) = -7.38 \pm 0.26 \text{ yr}^{-1}$.

To test for a spatial offset between the nebular emission and the stellar continuum, we extract profiles along the spatial axis of the NIRSpec MOS slit. We extract spatial profiles of the strong emission lines in $0.05 \mu\text{m}$ windows. For the stellar continuum, we extract the spatial profile of the spectrum at all wavelengths above $1.5 \mu\text{m}$, masking out the regions within $0.05 \mu\text{m}$ of any strong emission lines. We find no evidence for an offset between the nebular emission lines and stellar continuum (Figure S6).

We use the fluxes of the strongest emission lines of oxygen and hydrogen to estimate the oxygen abundance of the $z = 9.51$ galaxy. The high ratio $O_{32} \equiv F(\text{[O iii]})/F(\text{[O ii]}) = 13 \pm 4$ we calculate for this galaxy is consistent with highly ionized gas with low metallicity. We therefore use an empirical calibration (30) measured from low-metallicity ($12 + \log(\text{O/H}) \lesssim 8.0$) galaxies,

$$12 + \log(\text{O/H}) = 0.950 \log(R_{23} - 0.08O_{32}) + 6.805 \quad (2)$$

where $R_{23} \equiv (F(\text{[O ii] } 3727 \text{ \AA}) + F(\text{[O iii] } 4959 \text{ \AA}) + F(\text{[O iii] } 5007 \text{ \AA})) / F(\text{H}\beta)$. For the $z = 9.51$ galaxy, we find an oxygen abundance of $12 + \log(\text{O/H}) = 7.48 \pm 0.08$, where the uncertainty includes both line-flux and calibration uncertainties (21). Using alternative calibrations (31, 32) results in consistent estimates. The oxygen abundance derived from the photometry is also consistent (within 1.5σ) with the emission line calibrations (21).

Galaxy properties in context

The high magnification provided by gravitational lensing enabled us to detect this intrinsically faint galaxy ($M_{\text{UV},1500} = -17.4 \pm 0.22 \text{ mag}$), which has strong emission lines. Without lensing magnification, the galaxy's apparent magnitudes would be too faint to detect in the JWST images. We measured a lower mass and luminosity than other galaxies with strong emission line detections at $z > 7$, but a similar sSFR (Figure S4).

Star-forming galaxies that have emission lines with very large EWs at $z \lesssim 2.5$ exhibit tight correlations between the EW of the [O iii] 5007 Å emission line and the O_{32} ratio, and between the EWs of [O iii] 5007 Å and Hβ (37). The properties of the $z = 9.51$ galaxy are consistent with both of these

relations within 2σ (Figure S5). The high $O_{32} = 13 \pm 4$ we measure for this object is similar to that of other galaxies with high EW emission lines at high redshifts during the epoch of reionization, and of their local counterparts (38, 39). The high O_{32} might indicate a high escape fraction of hydrogen-ionizing radiation, f_{esc} . For example, using an empirical relation (40), we infer $f_{\text{esc}} = 0.65 \pm 0.45$. However, there is large scatter in this relation, and other methods of inferring f_{esc} do not yield such high escape fractions. For example, the UV spectral slope ($\beta = -1.98 \pm 0.11$) suggests a much smaller escape fraction, $f_{\text{esc}} = 0.035 \pm 0.011$ (41). Given these discrepant indicators and large uncertainties, we cannot draw any conclusions about f_{esc} from this galaxy.

The oxygen abundance is $12 + \log(\text{O/H}) = 7.48 \pm 0.08$ (see above), which is consistent (within 2σ) with the mass-metallicity relation observed in the local Universe for similar-mass galaxies (35). The galaxy's oxygen abundance is approximately 0.6 dex lower (2.5σ) than the more general relation between stellar mass, SFR, and metallicity (the fundamental metallicity relation; FMR) for dwarf galaxies at $z \sim 2 - 3$ (36) (Fig. 3). The oxygen abundances at redshift $z \gtrsim 3$ are known to fall below the FMR by 0.3 - 0.6 dex (42).

To determine whether the $z = 9.51$ galaxy hosts an active galactic nucleus (AGN), we compare our measurements of the stellar mass and the [O iii] 5007 Å to Hβ emission-line flux ratio ($\log\{F(\text{[O iii]})/F(\text{H}\beta)\} = 0.65 \pm 0.06$) to measurements from a sample of local galaxies at redshifts $0.04 < z < 0.2$ (44). At similar stellar masses and emission line ratios to the $z = 9.51$ galaxy, less than 1% of the local galaxies were classified as AGN. If this fraction does not substantially evolve with redshift, it is unlikely that the $z = 9.51$ galaxy hosts an AGN.

The half-light radius we measure for this galaxy, $R_e = 16.2_{-7.2}^{+4.6} \text{ pc}$, is very compact compared to galaxies with similar luminosities at redshifts $z = 6$ to 8 (Fig. 4). The half-light radius of the $z = 9.51$ galaxy is a factor of $9.8_{-2.6}^{+6.5}$ times smaller than the size-luminosity relation at those redshifts (43), a 4σ difference. The galaxy is also more compact than individual star-forming clumps with similar SFRs observed at redshifts $1 < z < 8$ (45) (Figure S9). Star-forming clumps have been shown to have a trend of increasing SFR at a fixed size with increasing redshift (46).

From our measurements of the SFR and half-light radius of the galaxy, we infer a very high star formation rate surface density $\sum_{\text{SFR}} 1190_{-580}^{+2440} M_\odot \text{ yr}^{-1} \text{ kpc}^{-2}$. Σ_{SFR} has been observed to increase with redshift from $z \sim 0$ to ~ 8 (47). The Σ_{SFR} of the $z = 9.51$ galaxy is a factor of 38_{-11}^{+129} times higher than the galaxies in the highest redshift bin ($z \sim 8$) of that sample (Figure S8).

REFERENCES AND NOTES

- N. Aghanim, Y. Akrami, M. Ashdown, J. Aumont, C. Baccigalupi, M. Ballardini, A. J. Banday, R. B. Barreiro, N. Bartolo, S. Basak, R. Battye, K. Benabed, J.-P. Bernard, M. Bersanelli, P. Bielewicz, J. J. Bock, J. R. Bond, J. Borrill, F. R. Bouchet, F. Boulanger, M. Bucher, C. Burigana, R. C. Butler, E. Calabrese, J.-F. Cardoso, J. Carron, A. Challinor, H. C. Chiang, J. Chluba, L. P. L. Colombo, C. Combet, D. Contreras, B. P. Crill, F. Cuttaia, P. de Bernardis, G. de Zotti, J. Delabrouille, J.-M. Delouis, E. Di Valentino, J. M. Diego, O. Doré, M. Douspis, A. Ducout, X. Dupac, S. Dusini, G. Efstathiou, F. Elsner, T. A. Enßlin, H. K. Eriksen, Y. Fantaye, M. Farhang, J. Fergusson, R. Fernandez-Cobos, F. Finelli, F. Forastieri, M. Frailis, A. A. Fraisse, E. Franceschi, A. Frolov, S. Galeotta, S. Galli, K. Ganga, R. T. Génova-Santos, M. Gerbino, T. Ghosh, J. González-Nuevo, K. M. Górski, S. Gratton, A. Gruppuso, J. E. Gudmundsson, J. Hamann, W. Handley, F. K. Hansen, D. Herranz, S. R. Hildebrandt, E. Hivon, Z. Huang, A. H. Jaffe, W. C. Jones, A. Karakci, E. Keihänen, R. Keskitalo, K. Kiiveri, J. Kim, T. S. Kisner, L. Knox, N. Krachmalnicoff, M. Kunz, H. Kurki-Suonio, G. Lagache, J.-M. Lamarre, A. Lasenby, M. Lattanzi, C. R. Lawrence, M. Le Jeune, P. Lemos, J. Lesgourgues, F. Levrier, A. Lewis, M. Liguori, P. B. Lilje, M. Lilley, V. Lindholm, M. López-Caniego, P. M. Lubin, Y.-Z. Ma, J. F. Macías-Pérez, G. Maggio, D. Maino, N. Mandolesi, A. Mangilli, A. Marcos-Caballero, M. Maris, P. G. Martin, M. Martinelli, E. Martínez-González, S. Matarrese, N. Mauri, J. D. McEwen, P. R. Meinhold, A. Melchiorri, A. Mennella, M. Migliaccio, M. Millea, S. Mitra, M.-A. Miville-Deschénes, D. Molinari, L. Montier, G. Morgante, A. Moss, P. Natoli, H. U. Nørgaard-Nielsen, L. Pagano, D. Paoletti, B. Partridge, G. Patanchon, H. V. Peiris, F. Perrotta, V. Pettorino, F. Piacentini, L. Polastri, G. Polenta, J.-L. Puget, J. P. Rachen, M. Reinecke, M. Remazeilles, A. Renzi, G. Rocha, C. Rosset, G. Roudier, J. A. Rubiño-Martín, B. Ruiz-Granados, L. Salvati, M. Sandri, M. Savelainen, D. Scott, E. P. S. Shellard, C. Sirignano, G. Sirri, L. D. Spencer, R. Sunyaev, A.-S. Suur-Uiski, J. A. Tauber, D. Tavagnacco, M. Tenti, L. Toffolatti, M. Tomasi, T. Trombetti, L. Valenziano, J. Valiviita, B. Van Tent, L. Vibert, P. Vielva, F. Villa, N. Vittorio, B. D. Wandelt, I. K. Wehus, M. White, S. D. M. White, A. Zacchei, A. Zonca; Planck Collaboration, Planck 2018 results - VI. Cosmological parameters. *Astron. Astrophys.* **641**, A6 (2020). doi:[10.1051/0004-6361/201833910](https://doi.org/10.1051/0004-6361/201833910)
- S. L. Finkelstein, A. D'Aloisio, J.-P. Paardekooper, Russell Ryan Jr., P. Behroozi, K. Finlator, R. Livermore, P. R. U. Sanderbeck, C. D. Vecchia, S. Khochfar, Conditions for Reionizing the Universe with a Low Galaxy Ionizing Photon Escape Fraction. *Astrophys. J.* **879**, 36 (2019). doi:[10.3847/1538-4357/ab1ea8](https://doi.org/10.3847/1538-4357/ab1ea8)
- P. Dayal, Early galaxy formation and its large-scale effects. *Proc. Int. Astron. Union* **15** (S352), 43–43 (2019). doi:[10.1017/S1743921320000106](https://doi.org/10.1017/S1743921320000106)
- B. E. Robertson, S. R. Furlanetto, E. Schneider, S. Charlot, R. S. Ellis, D. P. Stark, R. J. McLure, J. S. Dunlop, A. Koekemoer, M. A. Schenker, M. Ouchi, Y. Ono, E. Curtis-Lake, A. B. Rogers, R. A. A. Bowler, M. Cirasuolo, New Constraints ON Cosmic Reionization from the 2012 Hubble Ultra Deep Field Campaign. *Astrophys. J.* **768**, 71 (2013). doi:[10.1088/0004-637X/768/1/71](https://doi.org/10.1088/0004-637X/768/1/71)
- N. J. Adams, C. J. Conselice, L. Ferreira, D. Austin, J. A. Trussler, I. Juodžbalis, S. M. Wilkins, J. Caruana, P. Dayal, A. Verma, A. P. Vijayan, Discovery and properties of ultra-high redshift galaxies ($9 < z < 12$) in the JWST ERO SMACS 0723 Field. *Mon. Not. R. Astron. Soc.* **518**, 4755–4766 (2022). doi:[10.1093/mnras/stac3347](https://doi.org/10.1093/mnras/stac3347)
- M. Castellano, A. Fontana, T. Treu, P. Santini, E. Merlin, N. Leethochawalit, M. Trenti, E. Vanzella, U. Mestric, A. Bonchi, D. Belfiori, M. Nonino, D. Paris, G. Polenta, G. Roberts-Borsani, K. Boyett, M. Bradač, A. Calabro, K. Glazebrook, C. Grillo, S. Mascia, C. Mason, A. Mercurio, T. Morishita, T. Nanayakkara, L. Pentericci, P. Rosati, B. Vulcani, X. Wang, L. Yang, Early Results from GLASS-JWST. III. Galaxy Candidates at $z \sim 9 - 15^*$. *Astrophys. J. Lett.* **938**, L15 (2022). doi:[10.3847/2041-8213/ac94d0](https://doi.org/10.3847/2041-8213/ac94d0)
- H. Yan, Z. Ma, C. Ling, C. Cheng, J.-S. Huang, First Batch of $z \sim 11 - 20$. *Astrophys. J. Lett.* **942**, L9 (2022). doi:[10.3847/2041-8213/aca80c](https://doi.org/10.3847/2041-8213/aca80c)
- H. Atek, M. Shuntov, L. J. Furtak, J. Richard, J.-P. Kneib, G. Mahler, A. Zitrin, H. J. McCracken, S. Charlot, J. Chevallard, I. Chemerynska, Revealing galaxy candidates out to $z \sim 16$ with JWST observations of the lensing cluster SMACS0723. *Mon. Not. R. Astron. Soc.* **519**, 1201–1220 (2022). doi:[10.1093/mnras/stac3144](https://doi.org/10.1093/mnras/stac3144)
- S. L. Finkelstein, M. B. Bagley, P. A. Haro, M. Dickinson, H. C. Ferguson, J. S. Kartaltepe, C. Papovich, D. Burgarella, D. D. Kocevski, M. Huertas-Company, K. G. Iyer, A. M. Koekemoer, R. L. Larson, P. G. Pérez-González, C. Rose, S. Tacchella, S. M. Wilkins, K. Chworowsky, A. Medrano, A. M. Morales, R. S. Somerville, L. Y. A. Yung, A. Fontana, M. Giavalisco, A. Grazian, N. A. Grogin, L. J. Kewley, A. Kirkpatrick, P. Kurczynski, J. M. Lotz, L. Pentericci, N. Pirzkal, S. Ravindranath, R. E. Ryan Jr., J. R. Trump, G. Yang, O. Almaini, R. O. Amorín, M. Annunziatella, B. E. Backhaus, G. Barro, P. Behroozi, E. F. Bell, R. Bhatawdekar, L. Bisigello, V. Bromm, V. Buat, F. Buitrago, A. Calabro, C. M. Casey, M. Castellano, Ó. A. Chávez Ortiz, L. Ciesla, N. J. Cleri, S. H. Cohen, J. W. Cole, K. C. Cooke, M. C. Cooper, A. R. Cooray, L. Costantin, I. G. Cox, D. Croton, E. Daddi, R. Davé, A. de la Vega, A. Dekel, D. Elbaz, V. Estrada-Carpenter, S. M. Faber, V. Fernández, K. D. Finkelstein, J. Freundlich, S. Fujimoto, Á. García-Argumánez, J. P. Gardner, E. Gawiser, C. Gómez-Guijarro, Y. Guo, K. Hamblin, T. S. Hamilton, N. P. Hathi, B. W. Holwerda, M. Hirschmann, T. A. Hutchison, A. E. Jaskot, S. W. Jha, S. Jogee, S. Juneau, I. Jung, S. A. Kassin, A. L. Bail, G. C. K. Leung, R. A. Lucas, B. Magnelli, K. B. Mantha, J. Matharu, E. J. McGrath, D. H. McIntosh, E. Merlin, B. Mobasher, J. A. Newman, D. C. Nicholls, V. Pandya, M. Rafelski, K. Ronayne, P. Santini, L.-M. Seillé, E. A. Shah, L. Shen, R. C. Simons, G. F. Snyder, E. R. Stanway, A. N. Straughn, H. I. Teplitz, B. N. Vanderhoof, J. Vega-Ferrero, W. Wang, B. J. Weiner, C. N. A. Willmer, S. Wuyts, J. A. Zavala, A Long Time Ago in a Galaxy Far, Far Away: A Candidate $z \sim 12$ Galaxy in Early JWST CEERS Imaging. *Astrophys. J. Lett.* **940**, L55 (2022). doi:[10.3847/2041-8213/ac966e](https://doi.org/10.3847/2041-8213/ac966e)
- R. P. Naidu, P. A. Oesch, P. Dokkum, E. J. Nelson, K. A. Suess, G. Brammer, K. E. Whitaker, G. Illingworth, R. Bouwens, S. Tacchella, J. Matthee, N. Allen, R. Bezanson, C. Conroy, I. Labbe, J. Leja, E. Leonova, D. Magee, S. H. Price, D. J. Setton, V. Strait, M. Stefanon, S. Toft, J. R. Weaver, A. Weibel, Two Remarkably Luminous Galaxy Candidates at $z \approx 10 - 12$ Revealed by JWST. *Astrophys. J. Lett.* **940**, L14 (2022). doi:[10.3847/2041-8213/ac9b22](https://doi.org/10.3847/2041-8213/ac9b22)
- I. Labb  , P. van Dokkum, E. Nelson, R. Bezanson, K. A. Suess, J. Leja, G. Brammer, K. Whitaker, E. Mathews, M. Stefanon, B. Wang, A population of red candidate massive galaxies ~ 600 Myr after the Big Bang. *Nature* (2023). doi:[10.1038/s41586-023-05786-2](https://doi.org/10.1038/s41586-023-05786-2) Medline
- C. A. Mason, M. Trenti, T. Treu, The brightest galaxies at cosmic dawn. *Mon. Not. R. Astron. Soc.* **521**, 497–503 (2023). doi:[10.1093/mnras/stad035](https://doi.org/10.1093/mnras/stad035)
- M. Boylan-Kolchin, Stress Testing Λ CDM with High-redshift Galaxy Candidates, *arXiv e-print*, arXiv:2208.01611 (2022).
- A. C. Carnall, R. Begley, D. J. McLeod, M. L. Hamadouche, C. T. Donnan, R. J. McLaren, J. S. Dunlop, B. Milvang-Jensen, C. L. Bondestam, F. Cullen, S. M. Jewell, C. L. Pollock, A first look at the SMACS 0723 JWST ERO: Spectroscopic redshifts, stellar masses, and star-formation histories. *Mon. Not. R. Astron. Soc. Lett.* **518**, L45–L50 (2022). doi:[10.1093/mnrasl/slac136](https://doi.org/10.1093/mnrasl/slac136)
- K. Z. Arellano-C  rdova, D. A. Berg, J. Chisholm, P. A. Haro, M. Dickinson, S. L. Finkelstein, F. Leclercq, N. S. J. Rogers, R. C. Simons, E. D. Skillman, J. R. Trump, J. S. Kartaltepe, A First Look at the Abundance Pattern—O/H, C/O, and Ne/O—in $z > 7$ Galaxies with JWST/NIRSpec. *Astrophys. J. Lett.* **940**, L23 (2022). doi:[10.3847/2041-8213/ac9ab2](https://doi.org/10.3847/2041-8213/ac9ab2)
- M. Curti, F. D'Eugenio, S. Carniani, R. Maiolino, L. Sandles, J. Witstok, W. M. Baker, J. S. Bennett, J. M. Piotrowska, S. Tacchella, S. Charlot, K. Nakajima, G. Maheson, F. Mannucci, A. Amiri, S. Arribas, F. Belfiore, N. R. Bonaventura, A. J. Bunker, J. Chevallard, G. Cresci, E. Curtis-Lake, C. Hayden-Pawson, G. C. Jones, N. Kumari, I. Laseter, T. J. Looser, A. Marconi, M. V. Maseda, J. Scholtz, R. Smit, H.   bler, I. E. Wallace, The chemical enrichment in the early Universe as probed by JWST via direct metallicity measurements at $z \sim 8$. *Mon. Not. R. Astron. Soc.* **518**, 425–438 (2022). doi:[10.1093/mnras/stac2737](https://doi.org/10.1093/mnras/stac2737)
- J. E. Rhoads, I. G. B. Wold, S. Harish, K. J. Kim, J. Pharo, S. Malhotra, A. Gabrielpillai, T. Jiang, H. Yang, Finding Peas in the Early Universe with JWST. *Astrophys. J. Lett.* **942**, L14 (2023). doi:[10.3847/2041-8213/acaaf](https://doi.org/10.3847/2041-8213/acaaf)
- D. Schaerer, R. Marques-Chaves, L. Barrufet, P. Oesch, Y. I. Izotov, R. Naidu, N. G. Guseva, G. Brammer, First look with JWST spectroscopy: Resemblance among $z \sim 8$ galaxies and local analogs. *Astron. Astrophys.* **665**, L4 (2022). doi:[10.1051/0004-6361/202244556](https://doi.org/10.1051/0004-6361/202244556)
- J. R. Trump, P. A. Haro, R. C. Simons, B. E. Backhaus, R. O. Amor  n, M. Dickinson, V. Fern  ndez, C. Papovich, D. C. Nicholls, L. J. Kewley, S. W. Brunker, J. J. Salzer, S. M. Wilkins, O. Almaini, M. B. Bagley, D. A. Berg, R. Bhatawdekar, L. Bisigello, V. Buat, D. Burgarella, A. Calabro, C. M. Casey, L. Ciesla, N. J. Cleri, J. W. Cole, M. C. Cooper, A. R. Cooray, L. Costantin, D. Croton, H. C. Ferguson, S. L. Finkelstein, S. Fujimoto, J. P. Gardner, E. Gawiser, M. Giavalisco, A. Grazian, N. A. Grogin, N. P. P.

- Hathi, M. Hirschmann, B. W. Holwerda, M. Huertas-Company, T. A. Hutchison, S. Jogee, S. Juneau, I. Jung, J. S. Kartaltepe, A. Kirkpatrick, D. D. Kocevski, A. M. Koekemoer, J. M. Lotz, R. A. Lucas, B. Magnelli, J. Matharu, P. G. Pérez-González, N. Pirzkal, M. Rafelski, C. Rose, L.-M. Seillé, R. S. Somerville, A. N. Straughn, S. Tacchella, B. N. Vanderhoof, B. J. Weiner, S. Wuyts, L. Y. A. Yung, J. A. Zavalá, The Physical Conditions of Emission-line Galaxies at Cosmic Dawn from JWST/NIRSpec Spectroscopy in the SMACS 0723 Early Release Observations. *Astrophys. J.* **945**, 35 (2023). doi:10.3847/1538-4357/acea8a
20. S. Fujimoto et al., CEERS Spectroscopic Confirmation of NIRCam-Selected $z > 8$ Galaxy Candidates with JWST/NIRSpec: Initial Characterization of their Properties. *arXiv e-prints*, arXiv:2301.09482 (2023).
21. Materials and methods are available as supplementary materials.
22. G. B. Brammer, P. G. van Dokkum, P. Coppi, EAZY: A Fast, Public Photometric Redshift Code. *Astrophys. J.* **686**, 1503–1513 (2008). doi:10.1086/591786
23. B. D. Johnson, J. Leja, C. Conroy, J. S. Speagle, Stellar Population Inference with Prospector. *Astrophys. J. Suppl. Ser.* **254**, 22 (2021). doi:10.3847/1538-4365/abef67
24. L. Yang, S. Birrer, T. Treu, A versatile tool for cluster lensing source reconstruction - I. Methodology and illustration on sources in the Hubble Frontier Field Cluster MACS J0717.5+3745. *Mon. Not. R. Astron. Soc.* **496**, 2648–2662 (2020). doi:10.1093/mnras/staa1649
25. S. Birrer, A. Shajib, D. Gilman, A. Galan, J. Aalbers, M. Millon, R. Morgan, G. Pagano, J. Park, L. Teodori, N. Tessore, M. Ueland, L. Van de Vyvere, S. Wagner-Carena, E. Wempe, L. Yang, X. Ding, T. Schmidt, D. Sluse, M. Zhang, A. Amara, lenstronomy II: A gravitational lensing software ecosystem. *J. Open Source Softw.* **6**, 3283 (2021). doi:10.21105/joss.03283
26. X. Ding, S. Birrer, T. Treu, J. D. Silverman, Galaxy shapes of Light (GaLight): a 2D modeling of galaxy images. *arXiv:2111.08721* (2021).
27. P. Jakobsen, P. Ferruit, C. Alves de Oliveira, S. Arribas, G. Bagnasco, R. Barbo, T. L. Beck, S. Birkmann, T. Böker, A. J. Bunker, S. Charlot, P. de Jong, G. de Marchi, R. Ehrenwinkler, M. Falcolini, R. Fels, M. Franx, D. Franz, M. Funke, G. Giardino, X. Gnata, W. Holota, K. Honnen, P. L. Jensen, M. Jentsch, T. Johnson, D. Jollet, H. Karl, G. Kling, J. Köhler, M.-G. Kolm, N. Kumari, M. E. Lander, R. Lemke, M. López-Caniego, N. Lützgendorf, R. Maiolino, E. Manjavacas, A. Marston, M. Maschmann, R. Maurer, B. Messerschmidt, S. H. Moseley, P. Mosner, D. B. Mott, J. Muzerolle, N. Pirzkal, J.-F. Pittet, A. Plitzke, W. Posselt, B. Rapp, B. J. Rauscher, T. Rawle, H.-W. Rix, A. Rödel, P. Rumler, E. Sabbi, J.-C. Salvignol, T. Schmid, M. Sirianni, C. Smith, P. Strada, M. te Plate, J. Valenti, T. Wettemann, T. Wiehe, M. Wiesmayer, C. J. Willott, R. Wright, P. Zeidler, C. Zincke, The Near-Infrared Spectrograph (NIRSpec) on the James Webb Space Telescope. *Astron. Astrophys.* **661**, A80 (2022). doi:10.1051/0004-6361/202142663
28. M. Cappellari, Full spectrum fitting with photometry in ppxf: non-parametric star formation history, metallicity and the quenching boundary from 3200 LEGA-C galaxies at redshift $z \sim 8$. *arXiv:2208.14974* (2022).
29. D. E. Osterbrock, *Astrophysics of gaseous nebulae and active galactic nuclei* (University Science Books, 1989).
30. Y. I. Izotov, N. G. Guseva, K. J. Fricke, C. Henkel, Low-redshift lowest-metallicity star-forming galaxies in the SDSS DR14. *Astron. Astrophys.* **623**, A40 (2019). doi:10.1051/0004-6361/201834768
31. R. Maiolino, T. Nagao, A. Grazian, F. Cocchia, A. Marconi, F. Mannucci, A. Cimatti, A. Pipino, S. Ballero, F. Calura, C. Chiappini, A. Fontana, G. L. Granato, F. Matteucci, G. Pastorini, L. Pentericci, G. Risaliti, M. Salvati, L. Silva, AMAZE. I. The evolution of the mass-metallicity relation at $z > 3$. *Astron. Astrophys.* **488**, 463–479 (2008). doi:10.1051/0004-6361/200809678
32. T. Jiang, S. Malhotra, J. E. Rhoads, H. Yang, Direct T_{e} Metallicity Calibration of R23 in Strong Line Emitters. *Astrophys. J.* **872**, 145 (2019). doi:10.3847/1538-4357/aaee8a
33. D. A. Berg, E. D. Skillman, A. R. Marble, L. van Zee, C. W. Engelbracht, J. C. Lee, R. C. Kennicutt Jr., D. Calzetti, D. A. Dale, B. D. Johnson, Direct Oxygen Abundances for Low-luminosity LVL Galaxies. *Astrophys. J.* **754**, 98 (2012). doi:10.1088/0004-637X/754/2/98
34. T. Hsyu, R. J. Cooke, J. X. Prochaska, M. Bolte, Searching for the Lowest-metallicity Galaxies in the Local Universe. *Astrophys. J.* **863**, 134 (2018). doi:10.3847/1538-4357/aad18a
35. Y.-H. Lin et al., Low Metallicity Galaxies from the Dark Energy Survey. *arXiv:2211.02094* (2022).
36. M. Li et al., The Mass-Metallicity Relation of Dwarf Galaxies at the Cosmic Noon in the JWST Era, *arXiv:2211.01382* (2022).
37. M. Tang, D. P. Stark, J. Chevallard, S. Charlot, MMT/MMIRS spectroscopy of $z = 1.3 - 2.4$ extreme [O iii] emitters: Implications for galaxies in the reionization era. *Mon. Not. R. Astron. Soc.* **489**, 2572–2594 (2019). doi:10.1093/mnras/stz2236
38. N. R. Eggen, C. Scarlata, E. Skillman, A. Jaskot, Blow-away in the Extreme Low-mass Starburst Galaxy Pox 186. *Astrophys. J.* **912**, 12 (2021). doi:10.3847/1538-4357/abe85d
39. S. R. Flury, A. E. Jaskot, H. C. Ferguson, G. Worseck, K. Makan, J. Chisholm, A. Saldana-Lopez, D. Schaerer, S. McCandliss, B. Wang, N. M. Ford, T. Heckman, Z. Ji, M. Giavalisco, R. Amorin, H. Atek, J. Blaizot, S. Borthakur, C. Carr, M. Castellano, S. Cristiani, S. De Barros, M. Dickinson, S. L. Finkelstein, B. Fleming, F. Fontanot, T. Garel, A. Grazian, M. Hayes, A. Henry, V. Mauerhofer, G. Micheva, M. S. Oey, G. Östlin, C. Papovich, L. Pentericci, S. Ravindranath, J. Rosdahl, M. Rutkowski, P. Santini, C. Scarlata, H. Teplitz, T. Thuan, M. Trebitsch, E. Vanzella, A. Verhamme, X. Xu, The Low-redshift Lyman Continuum Survey. I. New, Diverse Local Lyman Continuum Emitters. *Astrophys. J. Suppl. Ser.* **260**, 1 (2022). doi:10.3847/1538-4365/ac5331
40. Y. I. Izotov, D. Schaerer, G. Worseck, N. G. Guseva, T. X. Thuan, A. Verhamme, I. Orlitová, K. J. Fricke, J1154+2443: A low-redshift compact star-forming galaxy with a 46 per cent leakage of Lyman continuum photons. *Mon. Not. R. Astron. Soc.* **474**, 4514–4527 (2018). doi:10.1093/mnras/stx3115
41. J. Chisholm, A. Saldana-Lopez, S. Flury, D. Schaerer, A. Jaskot, R. Amorín, H. Atek, S. L. Finkelstein, B. Fleming, H. Ferguson, V. Fernández, M. Giavalisco, M. Hayes, T. Heckman, A. Henry, Z. Ji, R. Marques-Chaves, V. Mauerhofer, S. McCandliss, M. S. Oey, G. Östlin, M. Rutkowski, C. Scarlata, T. Thuan, M. Trebitsch, B. Wang, G. Worseck, X. Xu, The far-ultraviolet continuum slope as a Lyman Continuum escape estimator at high redshift. *Mon. Not. R. Astron. Soc.* **517**, 5104–5120 (2022). doi:10.1093/mnras/stac2874
42. P. Troncoso, R. Maiolino, V. Sommariva, G. Cresci, F. Mannucci, A. Marconi, M. Meneghetti, A. Grazian, A. Cimatti, A. Fontana, T. Nagao, L. Pentericci, Metallicity evolution, metallicity gradients, and gas fractions at $z \sim 3.4$. *Astron. Astrophys.* **563**, A58 (2014). doi:10.1051/0004-6361/201322099
43. R. J. Bouwens, G. D. Illingworth, P. G. van Dokkum, P. A. Oesch, M. Stefanon, B. Ribeiro, Sizes of Lensed Lower-luminosity $z = 4 - 8$ Galaxies from the Hubble Frontier Field Program. *Astrophys. J.* **927**, 81 (2022). doi:10.3847/1538-4357/ac4791
44. S. Juneau et al., Active galactic nuclei emission line diagnostics and the mass-metallicity relation up to redshift $z \sim 2$: The impact of selection effects and evolution. *Astrophys. J.* **788**, 88 (2014). doi:10.1088/0004-637X/788/1/88
45. A. Claeysens, A. Adamo, J. Richard, G. Mahler, M. Messa, M. Dessauges-Zavadsky, Star formation at the smallest scales: A JWST study of the clump populations in SMACS0723. *Mon. Not. R. Astron. Soc.* **520**, 2180–2203 (2023). doi:10.1093/mnras/stac3791
46. R. C. Livermore, T. A. Jones, J. Richard, R. G. Bower, A. M. Swinbank, T. T. Yuan, A. C. Edge, R. S. Ellis, L. J. Kewley, I. Smail, K. E. K. Coppin, H. Ebeling, Resolved spectroscopy of gravitationally lensed galaxies: Global dynamics and star-forming clumps on ~ 100 pc scales at $1 < z < 4$. *Mon. Not. R. Astron. Soc.* **450**, 1812–1835 (2015). doi:10.1093/mnras/stv686
47. T. Shibuya, M. Ouchi, Y. Harikane, Morphologies of $\sim 190,000$ galaxies at $z = 0 - 10$ revealed with HST legacy data. I. Size evolution. *Astrophys. J. Suppl. Ser.* **219**, 15 (2015). doi:10.1088/0067-0049/219/2/15
48. H. Bushouse et al., JWST Calibration Pipeline. Zenodo (2023). doi:10.5281/zenodo.7038885
49. M. L. Boyer, J. Anderson, M. Gennaro, M. Geha, K. B. Wingfield McQuinn, E. Tollerud, M. Correnti, M. J. Brenner Newman, R. E. Cohen, N. Kallivayalil, R. Beaton, A. A. Cole, A. Dolphin, J. S. Kalirai, K. M. Sandstrom, A. Savino, E. D. Skillman, D. R. Weisz, B. F. Williams, The JWST Resolved Stellar Populations Early Release Science Program. I. NIRCam Flux Calibration. *Res. Notes AAS* **6**, 191 (2022). doi:10.3847/2515-5172/ac923a
50. A. M. Koekemoer, S. M. Faber, H. C. Ferguson, N. A. Grogin, D. D. Kocevski, D. C. Koo, K. Lai, J. M. Lotz, R. A. Lucas, E. J. McGrath, S. Ogaz, A. Rajan, A. G. Riess, S. A. Rodney, L. Strolger, S. Casertano, M. Castellano, T. Dahlen, M. Dickinson, T.

- Dolch, A. Fontana, M. Giavalisco, A. Grazian, Y. Guo, N. P. Hathi, K.-H. Huang, A. van der Wel, H.-J. Yan, V. Acquaviva, D. M. Alexander, O. Almaini, M. L. N. Ashby, M. Barden, E. F. Bell, F. Bournaud, T. M. Brown, K. I. Caputi, P. Cassata, P. J. Challis, R.-R. Chary, E. Cheung, M. Cirasuolo, C. J. Conselice, A. R. Cooray, D. J. Croton, E. Daddi, R. Davé, D. F. de Mello, L. de Ravel, A. Dekel, J. L. Donley, J. S. Dunlop, A. A. Dutton, D. Elbaz, G. G. Fazio, A. V. Filippenko, S. L. Finkelstein, C. Frazer, J. P. Gardner, P. M. Garnavich, E. Gawiser, R. Gruetzbauch, W. G. Hartley, B. Häussler, J. Herrington, P. F. Hopkins, J.-S. Huang, S. W. Jha, A. Johnson, J. S. Kartaltepe, A. A. Khostovan, R. P. Kirshner, C. Lani, K.-S. Lee, W. Li, P. Madau, P. J. McCarthy, D. H. McIntosh, R. J. McLure, C. McPartland, B. Mobasher, H. Moreira, A. Mortlock, L. A. Moustakas, M. Mozena, K. Nandra, J. A. Newman, J. L. Nielsen, S. Niemi, K. G. Noeske, C. J. Papovich, L. Pentericci, A. Pope, J. R. Primack, S. Ravindranath, N. A. Reddy, A. Renzini, H.-W. Rix, A. R. Robaina, D. J. Rosario, P. Rosati, S. Salimbeni, C. Scarlata, B. Siana, L. Simard, J. Smidt, D. Snyder, R. S. Somerville, H. Spinrad, A. N. Straughn, O. Telford, H. I. Teplitz, J. R. Trump, C. Vargas, C. Villforth, C. R. Wagner, P. Wandro, R. H. Wechsler, B. J. Weiner, T. Wiklind, V. Wild, G. Wilson, S. Wuyts, M. S. Yun, CANDELS: The Cosmic Assembly Near-infrared Deep Extragalactic Legacy Survey—The Hubble Space Telescope Observations, Imaging Data Products, and Mosaics. *Astrophys. J. Suppl. Ser.* **197**, 36 (2011). doi:10.1088/0067-0049/197/2/36
51. Gaia Collaboration, The Gaia mission. *Astron. Astrophys.* **595**, A1 (2016). doi:10.1051/0004-6361/201629272
52. P. Gavras et al., Gaia Data Release 3: Cross-match of Gaia sources with variable objects from the literature. arXiv:2207.01946 [astro-ph.IM] (2022).
53. M. Postman, D. Coe, N. Benítez, L. Bradley, T. Broadhurst, M. Donahue, H. Ford, O. Graur, G. Graves, S. Jouvel, A. Koekemoer, D. Lemze, E. Medezinski, A. Molino, L. Moustakas, S. Ogaz, A. Riess, S. Rodney, P. Rosati, K. Umetsu, W. Zheng, A. Zitrin, M. Bartelmann, R. Bouwens, N. Czakon, S. Golwala, O. Host, L. Infante, S. Jha, Y. Jimenez-Teja, D. Kelson, O. Lahav, R. Lazkoz, D. Maoz, C. McCully, P. Melchior, M. Meneghetti, J. Merten, J. Moustakas, M. Nonino, B. Patel, E. Regös, J. Sayers, S. Seitz, A. Van der Wel, The Cluster Lensing and Supernova Survey with Hubble: An Overview. *Astrophys. J. Suppl. Ser.* **199**, 25 (2012). doi:10.1088/0067-0049/199/2/25
54. M. Nonino, M. Dickinson, P. Rosati, A. Grazian, N. Reddy, S. Cristiani, M. Giavalisco, H. Kuntschner, E. Vanzella, E. Daddi, R. A. E. Fosbury, C. Cesarsky, Deep U band and R imaging of GOODS-South: Observations, data reduction, and first results. *Astrophys. J. Suppl. Ser.* **183**, 244–260 (2009). doi:10.1088/0067-0049/183/2/244
55. E. Bertin et al., *Astronomical Data Analysis Software and Systems XI*, D. A. Bohlender, D. Durand, T. H. Handley, eds. (2002), vol. 281 of *Astronomical Society of the Pacific Conference Series*, p. 228.
56. E. Bertin, *Astronomical Data Analysis Software and Systems XV*, C. Gabriel, C. Arviset, D. Ponz, S. Enrique, eds. (2006), vol. 351 of *Astronomical Society of the Pacific Conference Series*, p. 112.
57. G. Brammer, Grizli: Grism redshift and line analysis software, ascl:1905.001 (Astrophysics Source Code Library, 2019).
58. K. Horne, An optimal extraction algorithm for CCD spectroscopy. *Publ. Astron. Soc. Pac.* **98**, 609–617 (1986). doi:10.1086/131801
59. P. Sánchez-Blázquez, R. F. Peletier, J. Jimenez-Vicente, N. Cardiel, A. J. Cenarro, J. Falcon-Barroso, J. Gorgas, S. Selam, A. Vazdekis, Medium-resolution Isaac Newton Telescope library of empirical spectra. *Mon. Not. R. Astron. Soc.* **371**, 703–718 (2006). doi:10.1111/j.1365-2966.2006.10699.x
60. J. Falcón-Barroso, P. Sánchez-Blázquez, A. Vazdekis, E. Ricciardelli, N. Cardiel, A. J. Cenarro, J. Gorgas, R. F. Peletier, An updated MILES stellar library and stellar population models. *Astron. Astrophys.* **532**, A95 (2011). doi:10.1051/0004-6361/201116842
61. P. Virtanen, R. Gommers, T. E. Oliphant, M. Haberland, T. Reddy, D. Cournapeau, E. Burovski, P. Peterson, W. Weckesser, J. Bright, S. J. van der Walt, M. Brett, J. Wilson, K. J. Millman, N. Mayorov, A. R. J. Nelson, E. Jones, R. Kern, E. Larson, C. J. Carey, Í. Polat, Y. Feng, E. W. Moore, J. VanderPlas, D. Laxalde, J. Perktold, R. Cimrman, I. Henriksen, E. A. Quintero, C. R. Harris, A. M. Archibald, A. H. Ribeiro, F. Pedregosa, P. van Mulbregt, SciPy 1.0 Contributors, SciPy 1.0: Fundamental algorithms for scientific computing in Python. *Nat. Methods* **17**, 261–272 (2020). doi:10.1038/s41592-019-0686-2 Medline
62. P. J. Storey, C. J. Zeippen, Theoretical values for the [O iii] 5007/4959 line-intensity ratio and homologous cases. *Mon. Not. R. Astron. Soc.* **312**, 813–816 (2000). doi:10.1046/j.1365-8711.2000.03184.x
63. G. Chabrier, Galactic Stellar and Substellar Initial Mass Function. *Publ. Astron. Soc. Pac.* **115**, 763–795 (2003). doi:10.1086/376392
64. C. Conroy, J. E. Gunn, M. White, The Propagation of Uncertainties in Stellar Population Synthesis Modeling. I. The Relevance of Uncertain Aspects of Stellar Evolution and the Initial Mass Function to the Derived Physical Properties of Galaxies. *Astrophys. J.* **699**, 486–506 (2009). doi:10.1088/0004-637X/699/1/486
65. C. Conroy, J. E. Gunn, The Propagation of Uncertainties in Stellar Population Synthesis Modeling. III. Model Calibration, Comparison, and Evaluation. *Astrophys. J.* **712**, 833–857 (2010). doi:10.1088/0004-637X/712/2/833
66. J. S. Speagle, DYNESTY: A dynamic nested sampling package for estimating Bayesian posteriors and evidences. *Mon. Not. R. Astron. Soc.* **493**, 3132–3158 (2020). doi:10.1093/mnras/staa278
67. D. Langerood et al., Evolution of the Mass-Metallicity Relation from Redshift $z \approx 8$ to the Local Universe, arXiv:2212.02491 (2022).
68. P. Madau, Radiative Transfer in a Clumpy Universe: The Colors of High-Redshift Galaxies. *Astrophys. J.* **441**, 18 (1995). doi:10.1086/175332
69. M. Kriek, C. Conroy, The dust attenuation law in distant galaxies: Evidence for variation with spectral type. *Astrophys. J. Lett.* **775**, L16 (2013). doi:10.1088/2041-8205/775/1/L16
70. M. Oguri, The Mass Distribution of SDSS J1004+4112 Revisited. *Publ. Astron. Soc. Jpn.* **62**, 1017–1024 (2010). doi:10.1093/pasj/62.4.1017
71. M. Oguri, Fast Calculation of Gravitational Lensing Properties of Elliptical Navarro-Frenk-White and Hernquist Density Profiles. *Publ. Astron. Soc. Pac.* **133**, 074504 (2021). doi:10.1088/1538-3873/ac12dh
72. T. Okabe, M. Oguri, S. Peirani, Y. Suto, Y. Dubois, C. Pichon, T. Kitayama, S. Sasaki, T. Nishimichi, Shapes and alignments of dark matter haloes and their brightest cluster galaxies in 39 strong lensing clusters. *Mon. Not. R. Astron. Soc.* **496**, 2591–2604 (2020). doi:10.1093/mnras/staa1479
73. A. Zitrin, A. Fabris, J. Merten, P. Melchior, M. Meneghetti, A. Koekemoer, D. Coe, M. Maturi, M. Bartelmann, M. Postman, K. Umetsu, G. Seidel, I. Sendra, T. Broadhurst, I. Balestra, A. Biviano, C. Grillo, A. Mercurio, M. Nonino, P. Rosati, L. Bradley, M. Carrasco, M. Donahue, H. Ford, B. L. Frye, J. Moustakas, Hubble Space Telescope Combined Strong and Weak Lensing Analysis of the CLASH Sample: Mass and Magnification Models and Systematic Uncertainties. *Astrophys. J.* **801**, 44 (2015). doi:10.1088/0004-637X/801/1/44
74. J. Richard, G. P. Smith, J.-P. Kneib, R. S. Ellis, A. J. R. Sanderson, L. Pei, T. A. Targett, D. J. Sand, A. M. Swinbank, H. Dannerbauer, P. Mazzotta, M. Limousin, E. Egami, E. Jullo, V. Hamilton-Morris, S. M. Moran, LoCuSS: First results from strong-lensing analysis of 20 massive galaxy clusters at $z < 0.2$. *Mon. Not. R. Astron. Soc.* **404**, 325–349 (2010). doi:10.1111/j.1365-2966.2009.16274.x
75. G. B. Caminha, P. Rosati, C. Grillo, G. Rosani, K. I. Caputi, M. Meneghetti, A. Mercurio, I. Balestra, P. Bergamini, A. Biviano, M. Nonino, K. Umetsu, E. Vanzella, M. Annunziatella, T. Broadhurst, C. Delgado-Correal, R. Demarco, A. M. Koekemoer, M. Lombardi, C. Maier, M. Verdugo, A. Zitrin, Strong lensing models of eight CLASH clusters from extensive spectroscopy: Accurate total mass reconstructions in the cores. *Astron. Astrophys.* **632**, A36 (2019). doi:10.1051/0004-6361/201935454
76. J. F. Navarro, C. S. Frenk, S. D. M. White, A Universal Density Profile from Hierarchical Clustering. *Astrophys. J.* **490**, 493–508 (1997). doi:10.1086/304888
77. C. R. Keeton, A Catalog of Mass Models for Gravitational Lensing, arXiv:astro-ph/0102341 (2001).
78. R. Kawamata, M. Oguri, M. Ishigaki, K. Shimasaku, M. Ouchi, Precise Strong Lensing Mass Modeling of Four Hubble Frontier Field Clusters and a Sample of Magnified High-redshift Galaxies. *Astrophys. J.* **819**, 114 (2016). doi:10.3847/0004-637X/819/2/114
79. L. J. Furtak et al., UNCOVERing the extended strong lensing structures of Abell 2744 with the deepest JWST imaging, arXiv:2212.04318 (2022).
80. K. E. Heintz et al., A fundamental plane of galaxy assembly and chemical enrichment within the first 700 Myr after the Big Bang, arXiv:2212.02890 (2022).
81. R. L. Sanders, A. E. Shapley, N. A. Reddy, M. Kriek, B. Siana, A. L. Coil, B. Mobasher, I. Shivaei, W. R. Freeman, M. Azadi, S. H. Price, G. Leung, T. Fetherolf, L. de Groot,

- T. Zick, F. M. Fornasini, G. Barro, The MOSDEF survey: Direct-method metallicities and ISM conditions at $z \sim 1.5 - 3.5$. *Mon. Not. R. Astron. Soc.* **491**, 1427–1455 (2019). doi:10.1093/mnras/stz3032
82. R. L. Sanders, A. E. Shapley, M. Kriek, W. R. Freeman, N. A. Reddy, B. Siana, A. L. Coil, B. Mobasher, R. Davé, I. Shivaei, M. Azadi, S. H. Price, G. Leung, T. Fetherhoff, L. Groot, T. Zick, F. M. Fornasini, G. Barro, The MOSDEF Survey: A Stellar Mass-SFR-Metallicity Relation Exists at $z \sim 2.3$. *Astrophys. J.* **858**, 99 (2018). doi:10.3847/1538-4357/aabchd

ACKNOWLEDGMENTS

We thank Evan Skillman, Nathan Eggen, and Alexander Criswell for very helpful comments, and Sherry Suyu for assistance in obtaining the follow-up data. We thank program coordinator Tricia Royle, and instrument scientists Armin Rest, Diane Karakala, and Patrick Ogle of STScI for their help carrying out the HST observations. **Funding:** P.K. is supported by NSF grant AST-1908823 and STScI programs GO-15936, GO-16728 and GO-17253. M.O. acknowledges support by JSPS KAKENHI grants JP20H00181, JP20H05856, JP22H01260, and JP22K21349. T.T. acknowledges the support of NSF grant AST-1906976. R.J.F is supported in part by NSF grant AST-1815935, the Gordon & Betty Moore Foundation, and by a fellowship from the David and Lucile Packard Foundation. A.V.F. is grateful for financial assistance from the Christopher R. Redlich Fund. G.B. is funded by the Danish National Research Foundation (DNRF) under grant #140. A.Z. acknowledges support by Grant No. 2020750 from the United States-Israel Binational Science Foundation (BSF) and Grant No. 2109066 from the United States National Science Foundation (NSF), and by the Ministry of Science & Technology, Israel. J.H. and D.L. were supported by a VILLUM FONDEN Investigator grant (project number 16599). T.B. acknowledges support from the AEI under grant number PID2020-114035GB-100 and the Hong Kong Collaborative Research Fund under grant number C6017-20G. I.P.-F. and F.P. acknowledge support from the Spanish State Research Agency (AEI) under grant number PID2019-105552RB-C43. **Author contributions:** H.W. drafted the manuscript. H.W., P.K., C.S., N.R., T.T., and A.V.F. revised the manuscript. W.C. reduced the spectroscopy and H.W. analyzed the spectroscopy. C.S., Y.L., N.R., T.T., W.C., D.L., A.Z., L.Y., and T.B. contributed to the interpretation. T.T., W.C., A.V.F., R.J.F., J.H., A.M.K., L.S., J.P., T.B., S.J., G.B., S.S., I.P.F., F.P., and M.N. obtained JWST imaging. G.B. measured the photometry. M.O., A.Z., and J.M.D. modeled the gravitational lensing. **Competing interests:** We declare no competing interests. **Data and materials availability:** Raw HST imaging and JWST imaging and spectroscopy are available at <https://mast.stsci.edu> under Proposal IDs 02767 for JWST and 12457 for HST. Our reduced HST imaging, JWST imaging, and JWST spectroscopy are archived at Zenodo <https://zenodo.org/record/7767677>. Our measured photometry is provided in Table S1 and measured line fluxes in Table 1. The raw Subaru imaging is available at <https://smoka.nao.ac.jp/objectSearch.jsp> by selecting Suprime-Cam, then object RXJ2129+0005. **License information:** Copyright © 2023 the authors, some rights reserved; exclusive licensee American Association for the Advancement of Science. No claim to original US government works. <https://www.science.org/about/science-licenses-journal-article-reuse>

SUPPLEMENTARY MATERIALS

science.org/doi/10.1126/science.adf5307

Materials and Methods

Figs. S1 to S13

Tables S1 to S3

References (49–82)

Submitted 27 October 2022; accepted 28 March 2023

Published online 13 April 2023

10.1126/science.adf5307

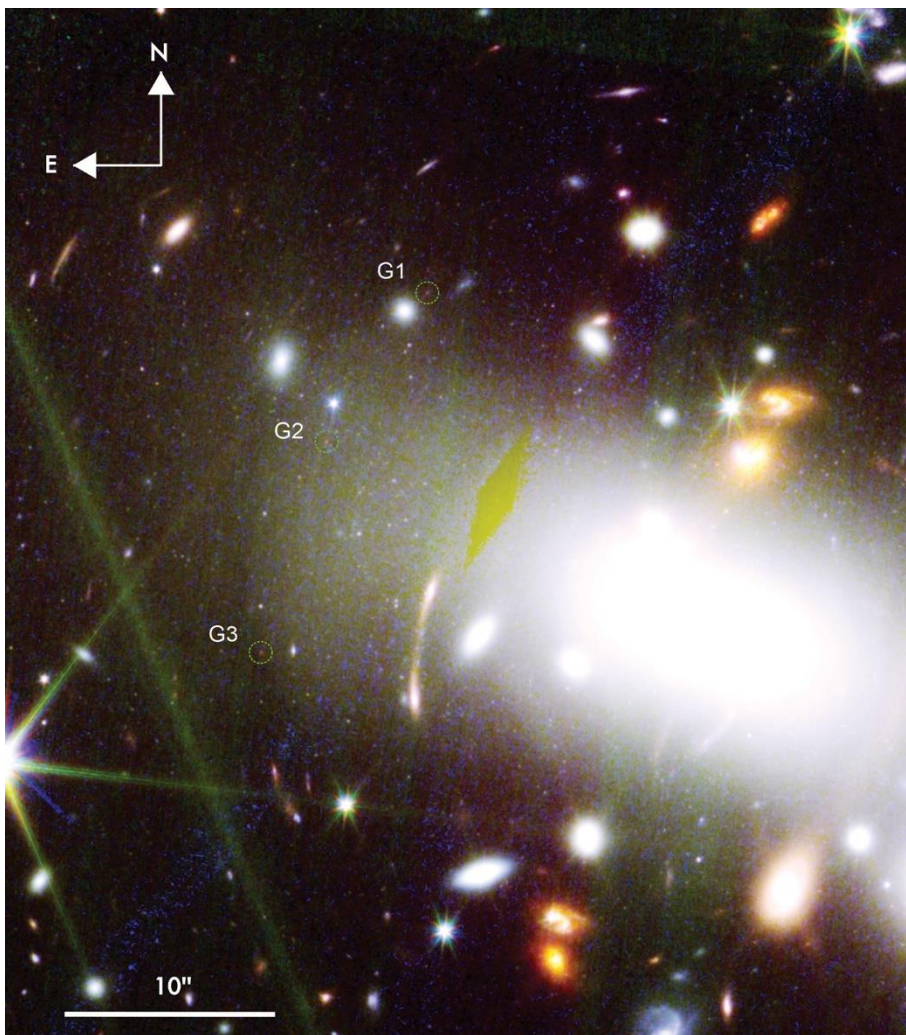


Fig. 1. Color-composite image of part of RX J2129. JWST NIRCam + HST ACS color-composite image of galaxy cluster RX J2129, with three images of the $z = 9.51$ galaxy circled in green. We obtained spectroscopy of image G2. Filters were assigned to RGB colors as: red JWST F277W+F356W+F444W; green JWST F115W+F150W+F200W; blue HST F606W + F814W. The broad blue and green bands are diffraction spikes caused by foreground stars. The yellow diamond is an artefact caused by a chip gap in the HST ACS camera. The individual red, green, and blue images are shown in Figures S11-S13.

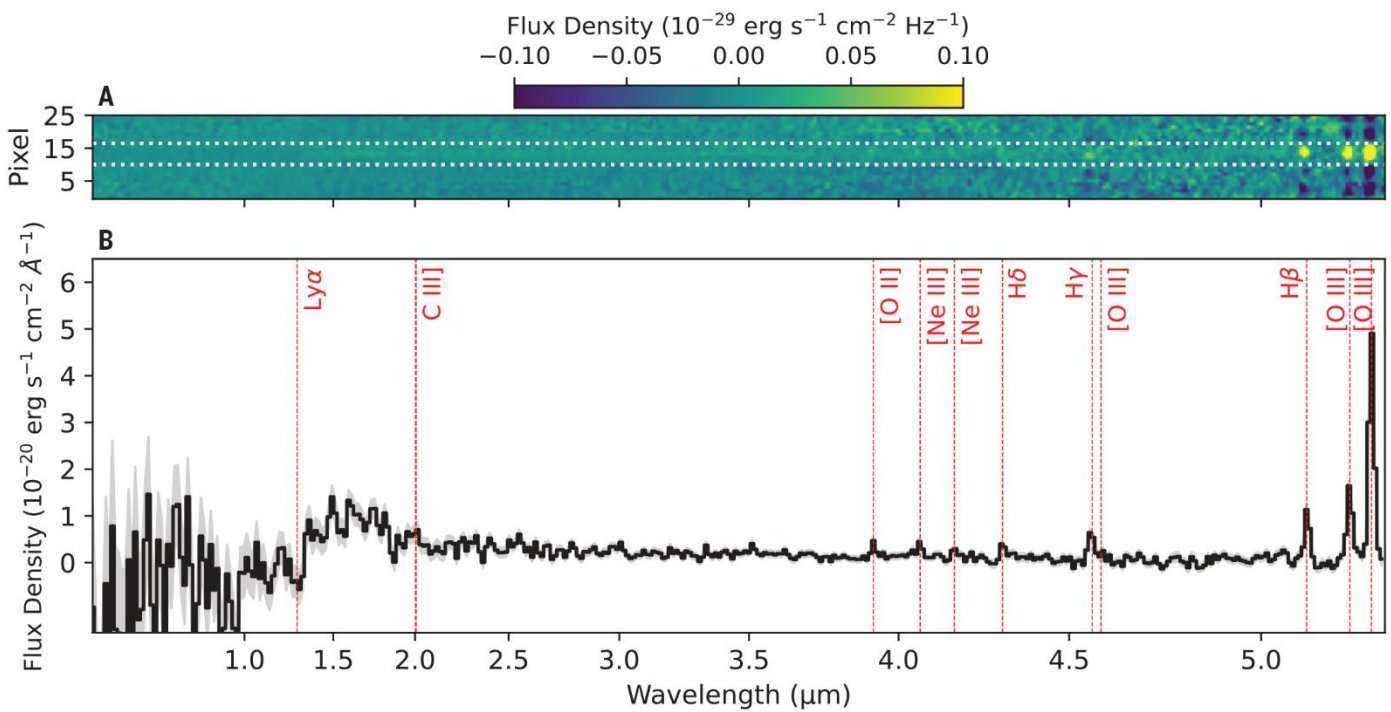


Fig. 2. Observed JWST spectrum of image G2. NIRSpec prism spectrum of image G2 of the $z = 9.51$ galaxy. This spectrum has not been corrected for magnification due to gravitational lensing. (A) Two dimensional spectrum, with flux densities indicated by the color bar. The apparent negative fluxes, in the background near the emission lines, are artefacts produced by the dither pattern used for the NIRSpec observations. The white dotted lines show the window used to extract the spectrum in (B). (B) One dimensional spectrum. The black line is the data, with gray shading indicating its 1σ uncertainties. Red vertical lines indicate the expected wavelengths of emission lines for $z = 9.51$.

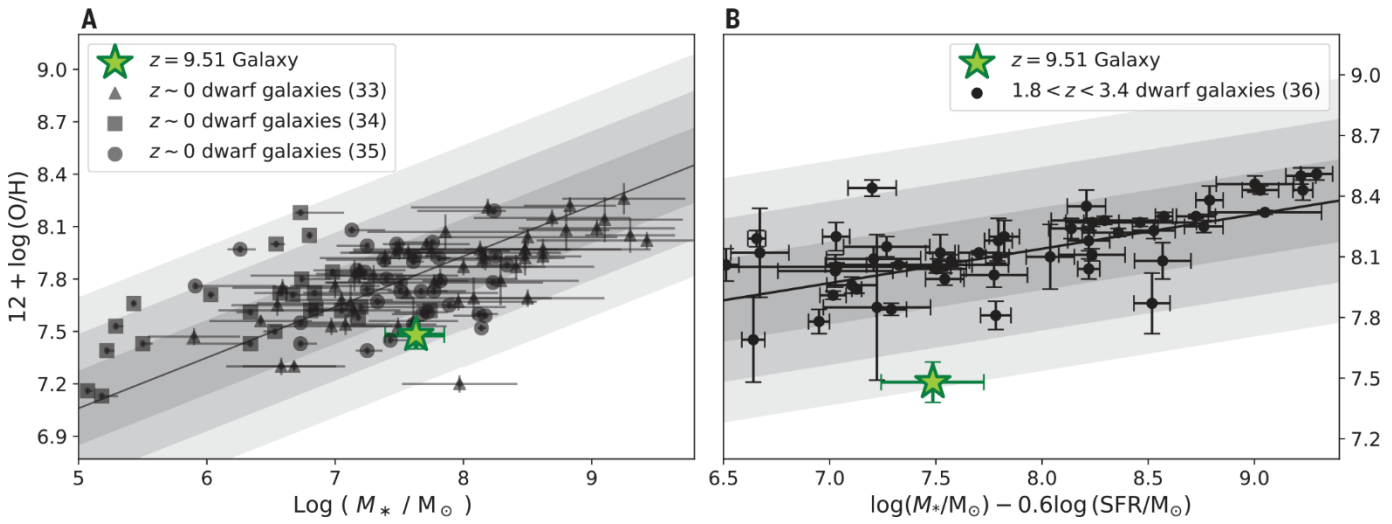


Fig. 3. Metallicity Relations. (A) The $z = 9.51$ galaxy (green star) compared to the mass-metallicity relation defined by local dwarf galaxies. Samples of local dwarfs are shown as black points (33–35) with error bars indicating 1σ uncertainties. The solid line is the mass-metallicity relation fitted to the triangle data points. Gray shading indicates, from dark to light, the 1σ , 2σ , and 3σ uncertainty ranges of this relation. (B) The more general fundamental metallicity relation (FMR) derived for dwarf galaxies at $z \sim 2 - 3$ (36). Plotting symbols are the same as panel A. The $z = 9.51$ galaxy falls 2.5σ below this relation.

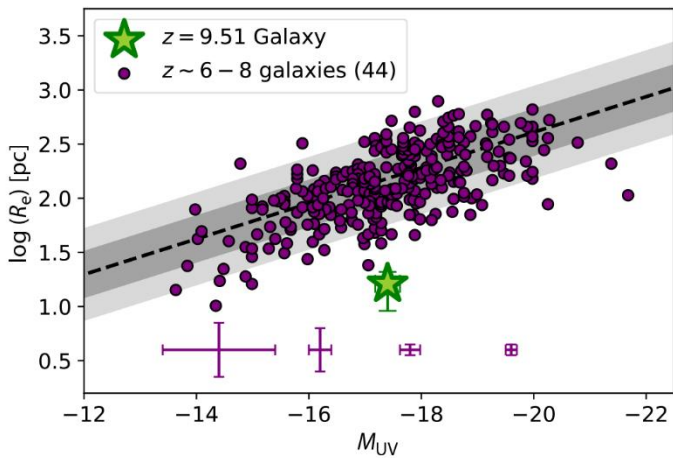


Fig. 4. Size-luminosity relation. The $z = 9.51$ galaxy (green star) compared to galaxies at redshifts $z \approx 6$ to 8 [purple circles (43)]. The half-light radius of the $z = 9.51$ galaxy is a factor of $9.3^{+10.5}_{-4.4}$ (3.5σ) smaller than the size-luminosity relation fitted to the purple points (43) (dashed line, with dark and light gray shaded regions indicating its 1σ and 2σ uncertainty ranges) The purple error bars indicate the typical 1σ uncertainties for the $z \approx 6$ to 8 galaxies at representative values of M_{UV} .

Table 1: Emission line flux measurements. Flux measurements and rest frame EWs of emission lines for the $z = 9.51$ galaxy. The flux measurements have not been corrected for magnification due to gravitational lensing. Upper limits are 3σ .

Emission line	Rest frame wavelength (\AA)	Observed flux ($10^{-19} \text{ erg s}^{-1} \text{ cm}^{-2}$)	Rest frame EW (\AA)
$\text{Ly}\alpha$	1216	< 39	< 31
$\text{C III}] + [\text{C III}]$	1907, 1909	< 20	< 51
$[\text{O II}]$	3626, 3629	5.9 ± 1.6	44 ± 12
$[\text{Ne III}]$	3869	6.3 ± 1.4	53 ± 12
$[\text{Ne III}] + \text{H}\varepsilon$	3968, 3970	< 4.9	< 39
$\text{H}\delta$	4102	5.7 ± 1.2	52 ± 11
$\text{H}\gamma$	4340	11.8 ± 1.7	195 ± 27
$[\text{O III}]$	4363	< 5.0	< 74
$\text{H}\beta$	4861	17.8 ± 2.5	248 ± 35
$[\text{O III}]$	4959	26.3 ± 1.8	392 ± 27
$[\text{O III}]$	5007	79.0 ± 2.0	1092 ± 28

A magnified compact galaxy at redshift 9.51 with strong nebular emission lines

Hayley Williams, Patrick L. Kelly, Wenlei Chen, Gabriel Brammer, Adi Zitrin, Tommaso Treu, Claudia Scarlata, Anton M. Koekemoer, Masamune Oguri, Yu-Heng Lin, Jose M. Diego, Mario Nonino, Jens Hjorth, Danial Langeroodi, Tom Broadhurst, Noah Rogers, Ismael Perez-Fournon, Ryan J. Foley, Saurabh Jha, Alexei V. Filippenko, Lou Strolger, Justin Pierel, Frederick Poidevin, and Lilan Yang

Science, **Ahead of Print**

DOI: 10.1126/science.adf5307

View the article online

<https://www.science.org/doi/10.1126/science.adf5307>

Permissions

<https://www.science.org/help/reprints-and-permissions>

Use of this article is subject to the [Terms of service](#)

Science (ISSN) is published by the American Association for the Advancement of Science. 1200 New York Avenue NW, Washington, DC 20005. The title *Science* is a registered trademark of AAAS.

Copyright © 2023 The Authors, some rights reserved; exclusive licensee American Association for the Advancement of Science. No claim to original U.S. Government Works